

Supplementary information

Multi-layered Alginate Hydrogel Structures and Bacteria Encapsulation

Yoon Jeong^{1,2} and Joseph Irudayaraj^{1,2,3*}

¹Department of Bioengineering, University of Illinois at Urbana-Champaign, Urbana, Illinois, USA

²Cancer Center at Illinois, University of Illinois at Urbana-Champaign, Urbana, Illinois, USA

³Carl R. Woese Institute for Genomic Biology, University of Illinois at Urbana-Champaign, Urbana, Illinois, USA

*Corresponding Author: (E-mail: jirudaya@illinois.edu)

Table of Contents

Experimental procedures -----	2
1. Fabrication of alginate core and hydrogel shell -----	2
2. Analytical Model for controlling the size of hydrogel core template -----	2
3. Bacteria encapsulation -----	2
4. Measurement of Bacteria density and Fluorescence intensity -----	3
5. Rheological test of Hydrogel bead -----	3
Supplementary Figs. S1 -----	4
Supplementary Figs. S2 -----	5
Supplementary Figs. S3 -----	6
Supplementary Figs. S4 -----	7
Supplementary Figs. S5 -----	8
Supplementary Figs. S6 -----	9
Supplementary Figs. S7 -----	10
Supplementary Figs. S8 -----	11
Supplementary Figs. S9 -----	12
References -----	13

Experimental procedures

1. Fabrication of alginate core and hydrogel shell

Alginate (Sigma/71238) solutions with concentrations in the range between 0.1-3 %wt were prepared in deionized (DI) water (resistance over 18 M Ω cm) and stored in refrigerated conditions (4°C) until further use. Alginate core beads were produced by a needle-based extrusion method by dropping alginate solution into 0.1M CaCl₂ (Sigma) solution under mild stirring. Briefly, sterile blunt needles ranging from 18 to 30 gauge were prepared, and the blunt needle was connected to a syringe to serve as a reservoir for alginate solutions. A syringe-pump system (Harvard Apparatus PHD 2000) was used at a constant flow infusion speed. A rotameter (Dwyer Instrument) was connected to a N₂ gas tubing line with the desired setting at a constant air-flow rate and the air outlet was positioned perpendicular to the end of the needle. The force required to detach an alginate droplet at the end of the needle was simply altered by adjusting the distance between the syringe needle and the air outlet. Alginate ionotropic gels were completely cross-linked depending on the size of the beads for 5-15 mins. The formed bead suspension was filtered using a 500-micron nylon mesh filter immersed in CaCl₂ solution to remove smaller size beads less than 500 μ m in diameter. The beads were placed on a nylon mesh of 200 μ m size to remove excess CaCl₂ solution and transferred to a very low concentration of alginate solution (less 0.1 wt%) prior to drying. Upon contact with a very low viscous solution, the concentration of the alginate solution increased immediately by up to 0.5 %wt. The reaction vessel containing the core beads was then aggressively shaken to prevent aggregation of the beads close to each other. The solution in the beaker was diluted by more than 20-fold by adding an excessive amount of DI water to arrest the interfacial reaction. Finally, the hydrogel-layered beads were washed three times with 0.05M CaCl₂ solution to stabilize the hydrogel layer and stored in DI water to prevent swelling or shrinkage. The size and thickness of the hydrogel beads was measured using an inverted microscope (Leica DMI3000B) equipped with a CCD camera (Qimaging EXi Blue).

2. Analytical Model for controlling the size of hydrogel core template

Theoretical approaches were used to control the size of core hydrogel beads described previously for analytical model development.¹ The relationship between the size of the core hydrogel beads and the process parameters was simplified based on an empirical model represented by Eqs. 1 and 2.

$$D_b = D_N (1 + m_{liq}/m_{air})^{X_n} [X_2 (Oh_{liq}/We_{air})^{X_1}] - \text{(eq 1)}$$

$$D_b = D_0 (1 - P_{liq-air})^{X_n} - \text{(eq 2)}$$

The mean diameter of alginate core beads (D_b) represented by the equation was correlated with the variables: X_n , X_0 , X_1 , and X_2 which are determined empirically. Experimental variables include needle diameter (D_N), mass flow ratio of liquid to air (m_{liq}/m_{air}), physical properties of liquid solution (Oh_{liq}), physical properties of air (We_{air}), diameter of alginate beads with no air pressure (D_0), and air pressurized at the air-liquid interface ($P_{liq-air}$). The non-linear parameter estimation and empirical data were analyzed using Origin 2019 (OriginLab).

3. Bacteria encapsulation

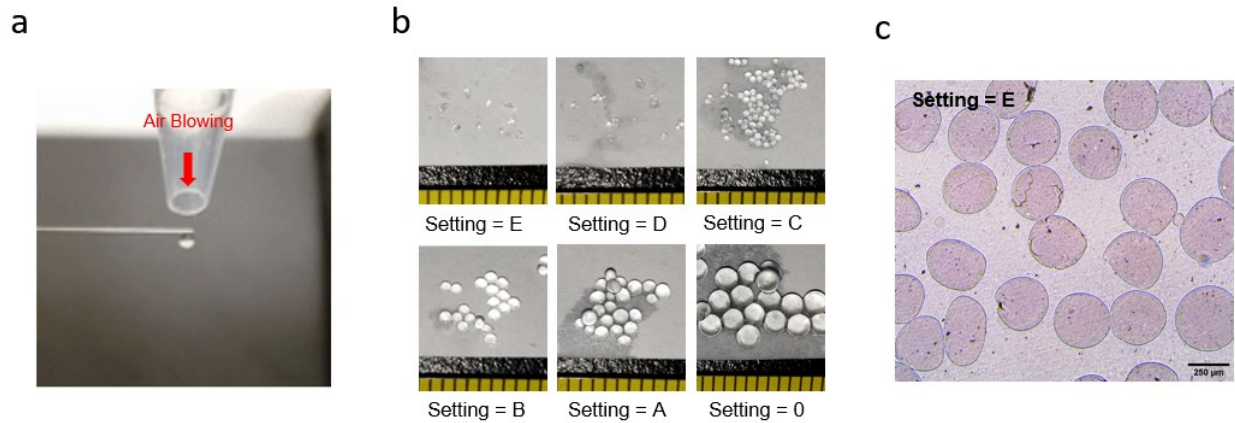
Escherichia coli DH5 α *pSmart-tet-kan-sfGFP* (*gfp E. coli*), thankfully provided from Dr. Vanderpool (University of Illinois Urbana-Champaign, USA), was grown in Luria-Bertani (LB) broth medium or LB agar plates (BD Difco, Miller) supplemented with 25 $\mu\text{g}/\text{mL}$ of kanamycin (Sigma) at 37°C. The bacteria concentration (OD₆₀₀, optical density 600 nm) was measured with a UV/vis spectrophotometer (Eppendorf Biophotometer) and the standard agar plate count method over the range of 30 to 300 CFU on a Petri dish. Aliquots were resuspended in fresh LB media to attain desired cell densities in the mid-exponential phase to obtain the necessary concentration prior to use in encapsulation experiments. Cultures at mid-exponential phase were mixed thoroughly with sterile alginate solution (3 wt%) for uniform distribution of cells. The cell-alginate mixture was dropped into a solution of 0.1M CaCl₂ under mild stirring through a conventional needle-based extrusion method (30G needles, BD PrecisionGlide™). After gelation for 10 mins, all other fabrication procedures were described as above. The formed beads containing bacteria with a hydrogel layer were washed with sterile DI water to remove excessive CaCl₂. Bacteria leakage test was conducted using two groups of *E. coli* encapsulated beads with/without the hydrogel layer. Cultured supernatant was measured by spectrophotometry (OD₆₀₀, optical density 600 nm).

4. Measurement of Bacteria density and Fluorescence intensity

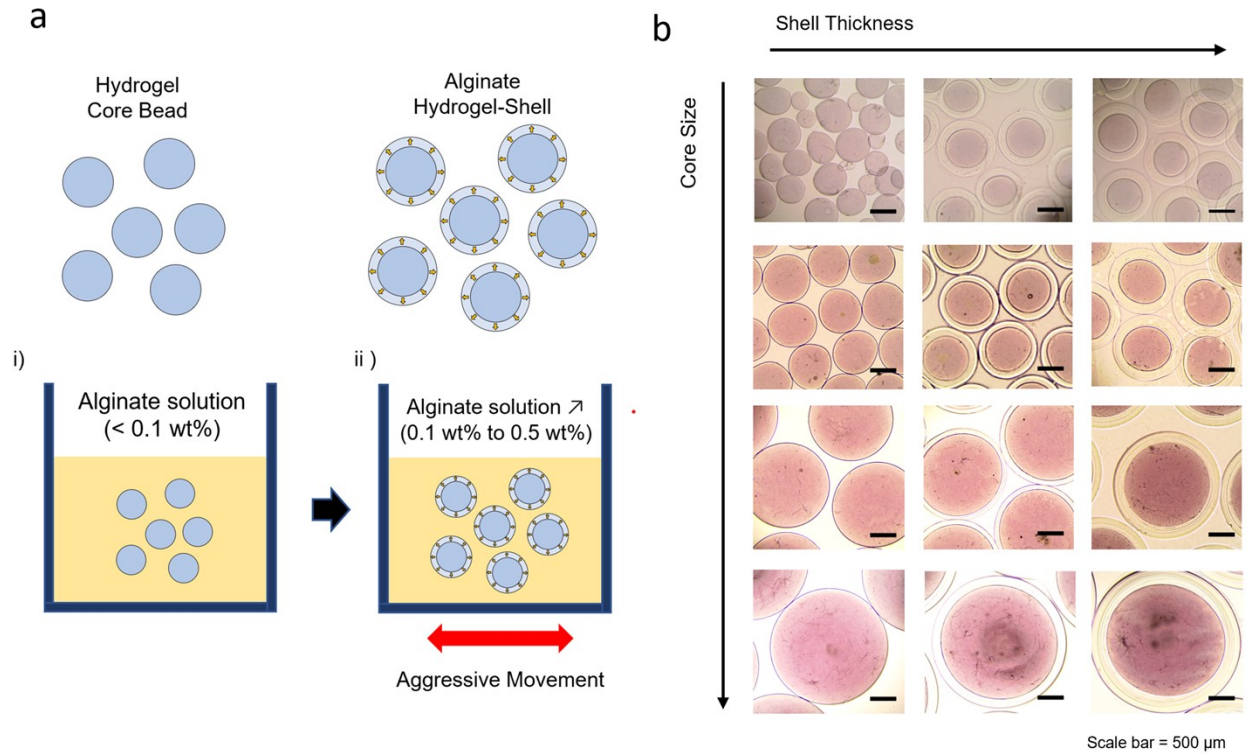
gfp E. coli beads were incubated in Luria-Bertani (LB) broth containing 25 $\mu\text{g}/\text{mL}$ of kanamycin at 37°C in 24 well plate. The bacterial concentrations of the *gfp E. coli* suspensions were pre-determined by the standard plate count method prior to use in hydrogel encapsulation. To estimate bacterial biomass in the *gfp E. coli* bead, cellular components at optical density 600 nm was measured by UV-vis spectrophotometry. Briefly, a *gfp E. coli* hydrogel bead was collected in a 1.5 ml sterile Eppendorf tube at each time point. The collected bead samples were degraded with 100 μl of 0.1 M sodium citrate (Sigma) in an Eppendorf tube. Then, 900 μl of fresh LB was added into the tube and OD 600 was measured by spectrometry. Fluorescence images of the samples were acquired using a Chemidoc XRS system (Bio-rad) with the 530/28 and 605/50 standard filter and analyzed using ImageJ software.

5. Rheological test of Hydrogel bead

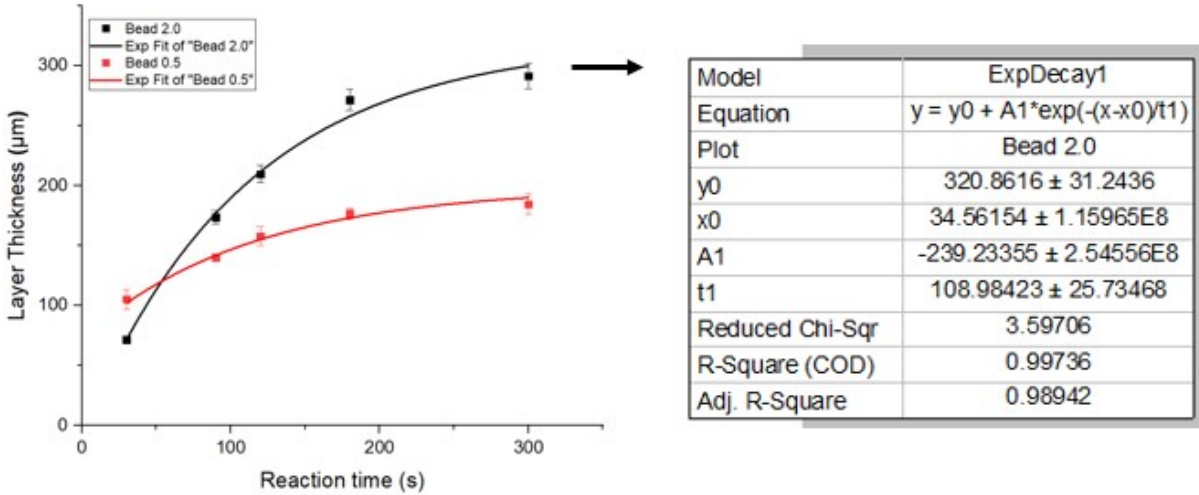
Rheological measurement of hydrogel samples was examined using a TA-XT2 analyzer (Texture Technologies Corp) with a 35-mm diameter probe.² Force-strain curves were recorded with the following test settings: 70% strain deformation, relaxation time of 5s, and force of 20g.



Supplementary Figure 1. **a**, An image of air-blowing needle-based air extrusion¹ for detaching an alginate droplet prior to ionotropic gelation in a gelling bath. **b**, Variation of the core bead size by air-extrusion fabrication. Alginate hydrogels in various sizes made by ionotropic gelation through controlling the air-blowing distance. **c**, Microscopic image of hydrogel beads, fabricated in the experimental setting E. The scale bar is 250 μm.



Supplemental Figure 2. **a**. Schematic illustration of alginate hydrogel-shell beads. Core beads were transferred together into a solution of alginate (less 0.1 wt%). Upon contact with a very low viscous solution, the concentration of the alginate solution increased immediately by up to 0.5 wt%. Immediate gelling at the interface between the outermost core begins as the excessive Ca^{2+} quickly diffuses from the alginate cores. The reaction vessel needs to be aggressively agitated to keep the core beads from sticking together. **b**. Microscope images of uniform hydrogel-layered beads over a range of sizes in different layer thickness. To remove small-size beads less than 500 μm in diameter (first row), the formed bead suspension was filtered using a 500-micron hole nylon mesh filter. The scale bar is 500 μm .



Supplemental Figure 3. Hydrogel layer gelation kinetics. The data were fit to an exponential model (left, Origin 9.0 software) used to derive the empirical based equation 1 and 2 of hydrogel thickness.³

$$H_t = H_\infty (1 - \alpha e^{-k_1 t}) \quad \alpha = e^{-k_2 t}$$

$$H_t = H_\infty (1 - e^{-(k_1 - k_2)t}) \quad k = k_1 - k_2$$

$$H_t = H_\infty (1 - e^{-kt}) \quad \text{---- (1)}$$

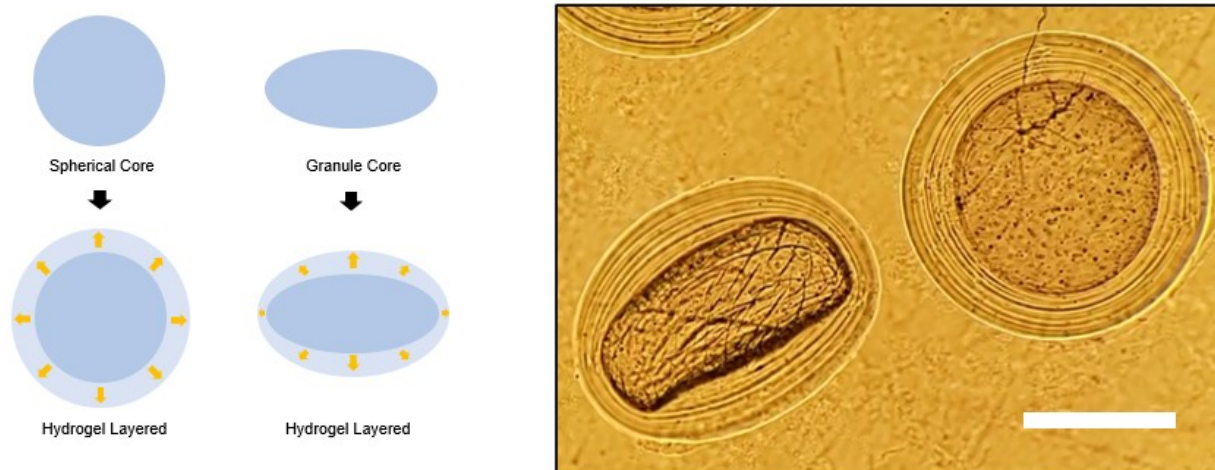
where H_t is the layer thickness at time t and H_∞ is the layer thickness at steady-state, and k is the rate constant of the gelation processes.

The reaction proceeds at a rate that depends on primarily the Ca^{2+} concentration at the gelling interface, following first order gelation kinetics.⁴

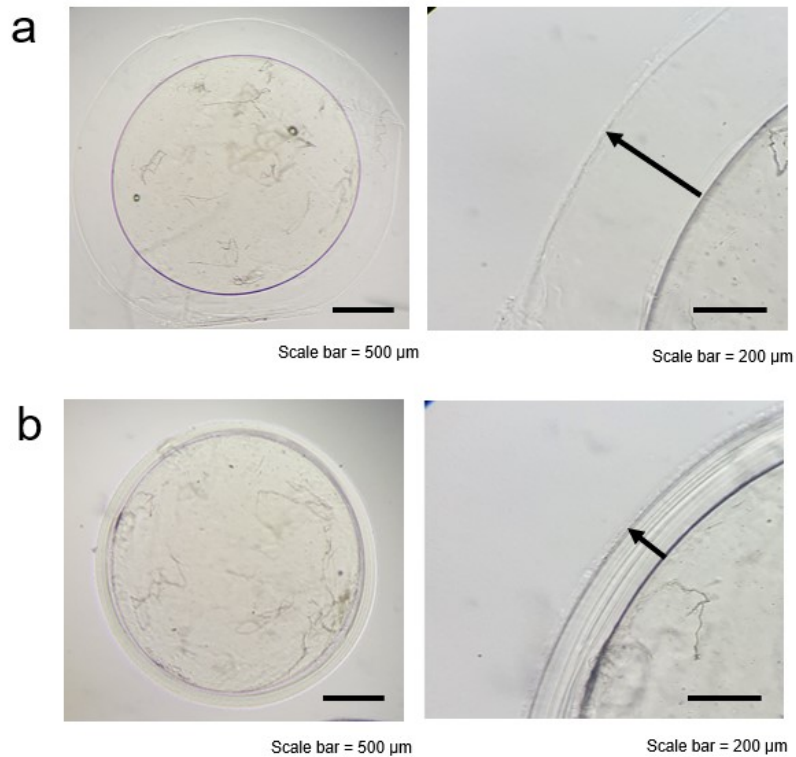
The general differential equation for the gelling kinetics based is given below.

$$\ln([A]_0/[A]_t) = kt \quad \text{---- (2)}$$

where $[A]$ is the concentration at time t and $[A]_0$ is the concentration at time 0, and k is the first-order rate constant.

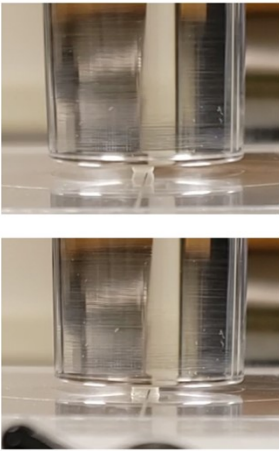


Supplemental Figure 4. The influence of core hydrogel morphological features in different gel layer thickness. Core morphological shape makes Ca^{2+} diffusion distance different, resulting in the fabrication of different hydrogel layer in thickness. Microscope comparison image of different shape hydrogel-layered beads. The scale bar is 500 μm .

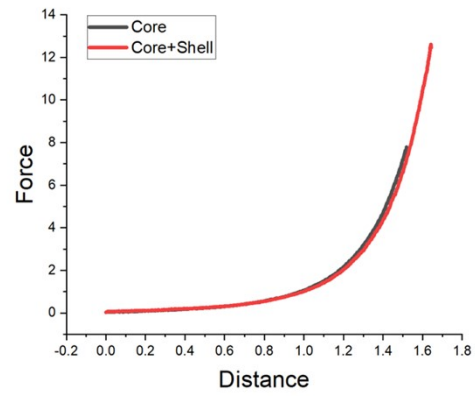


Supplemental Figure 5. The microscopic images of hydrogel layers fabricated under different conditions. **a**, Static condition **b**, Aggressive movement by the agitation process of a reaction vessel. The arrow indicates the outward direction of hydrogel gelling interface from the surface of core hydrogel.

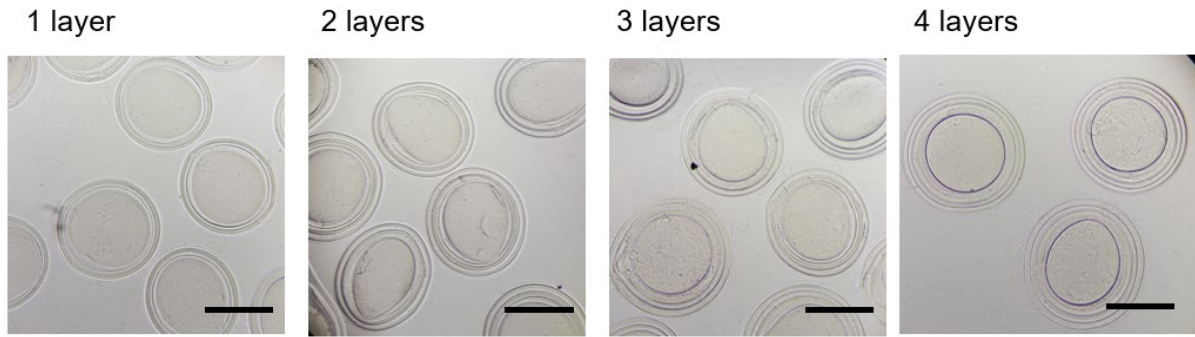
a



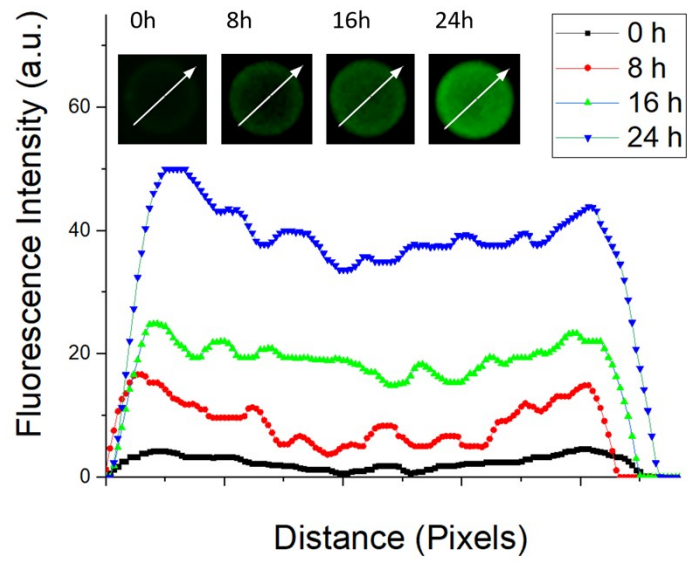
b



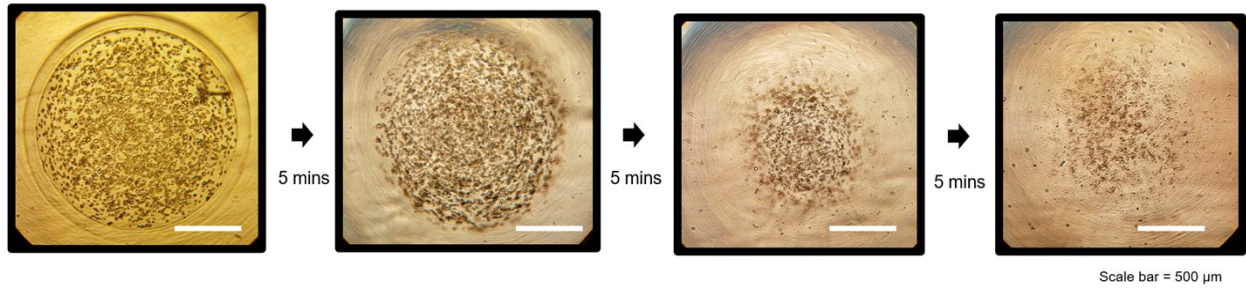
Supplemental Figure 6. Rheological analysis **a**. Compression mechanical properties of alginate core-shell bead **b**. Force - deformation curve by 70% strain.



Supplemental Figure 7. Representative microscopic images of multi-layered hydrogels. All alginate hydrogel layered beads with a uniform thickness were fabricated simultaneously in the same reaction vessel.
The scale bar is 500 μm.



Supplemental Figure 8. Fluorescence intensity profile of alginate hydrogel-shell beads with *gfp*-expressing *E. coli* for 24 hours.



Supplemental Figure 9. Degradation test of alginate core-shell hydrogel containing *E. coli*. 0.025M sodium citrate was used to accelerate degradation of the structures.

References

- 1 Lee, B. B., Bhandari, B. R. & Howes, T. Air extrusion system for ionotropic alginate microgel particle formation: a review. *Chemical Engineering & Technology* **39**, 2355-2369 (2016).
- 2 Yang, H., Irudayaraj, J., Otgonchimeg, S. & Walsh, M. Rheological study of starch and dairy ingredient-based food systems. *Food Chemistry* **86**, 571-578 (2004).
- 3 Zarket, B. C. & Raghavan, S. R. Onion-like multilayered polymer capsules synthesized by a bioinspired inside-out technique. *Nature communications* **8**, 1-10 (2017).
- 4 Grzybowski, B. A. *Chemistry in motion: reaction-diffusion systems for micro-and nanotechnology*. (John Wiley & Sons, 2009).